SUPPORTING INFORMATION

Energy framework and solubility: a new physicochemical approach in the evaluation of the structure-property of pharmaceutical solid forms

Jennifer T. J. Freitas[a], Luan F. Diniz[a,b], Daniele S. Gomes[a], Pedro M. A. F. de Paula[a], Sérgio H. A. de Castro[a], Larissa S. Martins[a], Daniely F. Silva[a], Ana L. M. Horta[a], Felipe A. S. Guimarães[a], Victória F. M. Calisto[a], Renata Diniz[a]*

[a]Grupo de Cristalografia Química (GCQ), Departamento de Química, Instituto de Ciências Exatas, Universidade Federal de Minas Gerais, 31270-901-Belo Horizonte, MG, Brazil.

[b]Laboratório de Controle de Qualidade de Medicamentos e Cosméticos, Departamento de Produtos Farmacêuticos, Faculdade de Farmácia, Universidade Federal de Minas Gerais, 31270-901, Belo Horizonte, MG, Brazil.

*E-mail: dinizr@ufmg.br

COMPLEMENTARY FIGURES AND TABLES

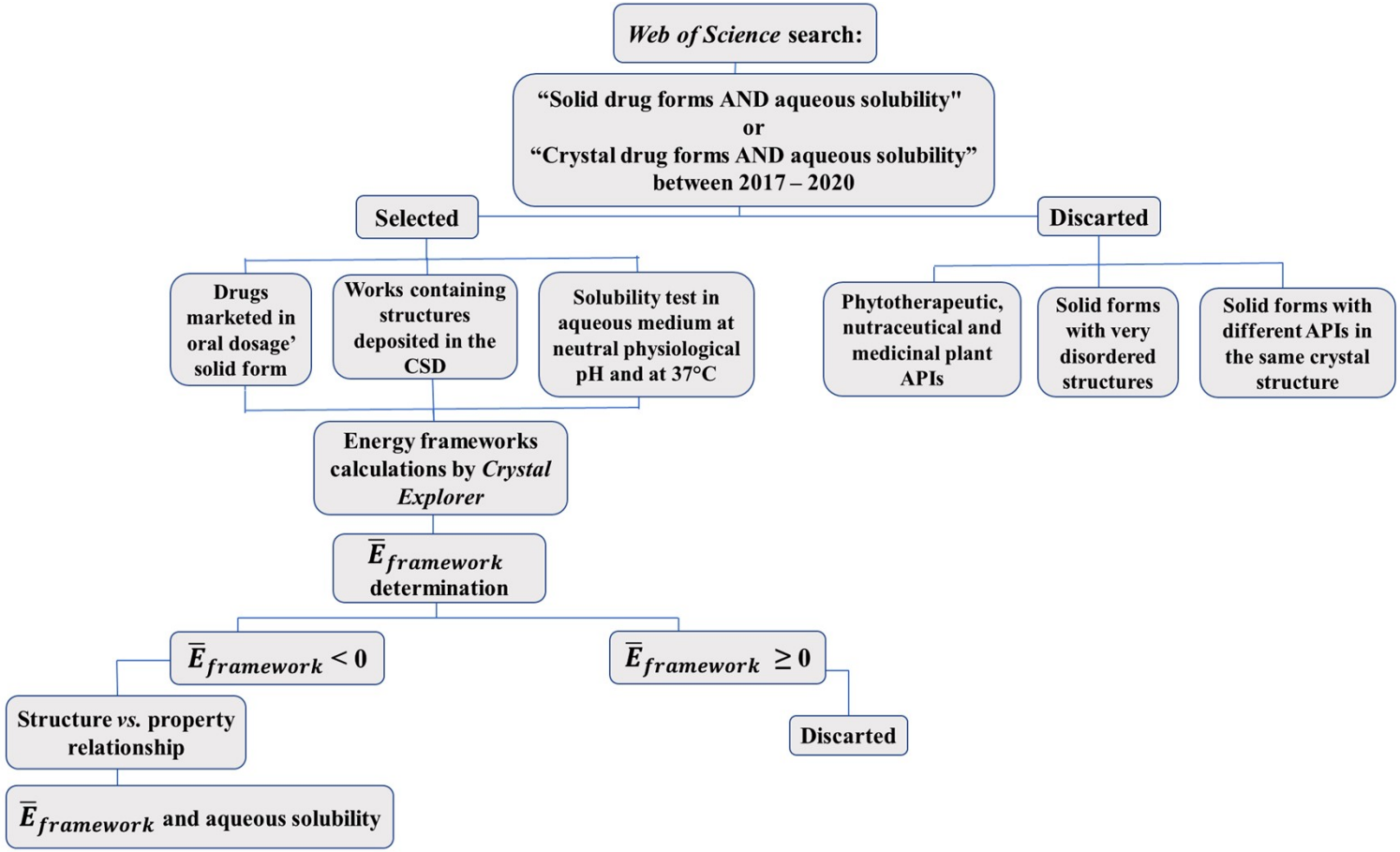

Figure S1. Steps of the methodology utilized in this work.

Table S1. Different solid forms selected for the analysis of structure-property correlation.

Drug	Solid form	Type of solid	Aqueous solubility (mg mL^{-1})*	HF $E_{framework}$ (KJ mol^{-1})	B3LYP $E_{framework}$ (KJ mol^{-1})	References
Acetozolamide (ACA)	ACA-form I	P	0.74	-27.44	-24.05	[1-2]
	ACA-proline	C	2.64	-15.5	-11.92	
	ACA-theophylline	C	2.18	-15.71	-16.33	
Albendazole (ABZ)	ABZ-form I	P	0.0033	-22.03	-22.04	[3]
	ABZ- hydrochloride	S	0.1	-11.09	-11.19	
Apatinib (APA)	APA- saccharinate	S	0.255	-9.58	-14.31	[4]
	APA-sebacylate	S	1.667	-14.84	-12.49	
	APA-succinate hydrated	S	0.989	-9.30	-13.94	
Apremilast (AP)	AP	P	0.004	-29.42	-25.07	[5]
Cilostazol (CLZ)	CLZ	P	0.0074	-28.56	-27.3	[6]
	CLZ-4-hydroxybenzoic acid	C	0.0703	-23.62	-23.08	
	CLZ-2,4-dihydroxybenzoic acid	C	0.1073	-23.79	-21.17	
	CLZ-2,5-dihydroxybenzoic acid	C	0.25382	-28.37	-26.37	
Chlorothiazide (CTZ)	CTZ-form 1	P	0.018	-28.07	-22.14	[7]
	CTZ-1,2-di(4-pyridyl)ethylene	C	0.028	-18.38	-12.27	
Doxazosin (DXZ)	DXZ - free-base	P	0.00006	-30.3	-28.36	[8]
	DXZ- mesylate polymorph A	S	0.0367	-12.14	-12.86	
	DXZ- mesylate hydrate	S	0.07434	-16.44	-14.08	
Desloratadine (DES)	DES	P	0.32	-20.83	-20.21	[9]

Dipfluzine (DF)	DF-fumarate	S	0.01911	-17.67	-20.25	[10]
Entacapone (ETP)	ETP	P	0.08	-31.73	-29.73	[11]
Epalrestat (EPR)	EPR	P	0.002956	-22.47	-21.27	[12-13]
	EPR-caffeine	C	0.004557	-15.78	-19.05	
Febuxostat (FEB)	FEB- isonicotinamide	C	0.0131	-18.78	-18.73	[14-16]
	HFEB-di-2-pyridylamine	S	0.1419	-7.52	-8.78	
	FEB	P	0.0108	-20.89	-20.00	
Furosemide (FSM)	FSM-form 1	P	0.081	-10.83	-9.07	[17-18]
	FSM-5-fluorocytosine monohydrated	C	0.22	-22.96	-21.92	
	FSM-triethanolamine	S	4.3	-7.75	-10.18	
Glibenclamide (GCM)	GCM	P	0.0101	-27.99	-25.72	[19]
Glimepiride (GLIM)	GLIM- form I	P	0.0464	-35.63	-32.73	[20]
	GLIM- form II	P	0.133	-37.47	-33.67	
Indomethacin (INC)	INC-DL-proline hydrate	C	0.00377	-24.81	-25.32	[21-22]
	INC- polymorph γ	P	0.00186	-26.56	-24.99	
	$(INC)_2$ -$(DPEN)_2$-Dihydrate	C	0.3598	-1.83	-4.28	
Ketoconazole (KTZ)	KTZ	P	0.012	-31.78	-30.82	[23]
	KTZ-2,4 dihydroxybenzoic acid	C	0.1793	-17.11	-16.784	
	KTZ-3,4-dihydroxybenzoic acid	C	0.4858	-24.12	-21.83	
	KTZ-*trans*-4-hydroxycinnamic acid	C	0.0815	-26.80	-24.55	
Leflunomide (LEF)	LEF-form I	P	0.03165	-26.74	-24.85	[24]
	LEF-3-hydroxybenxoic acid	C	0.03658	-20.46	-18.08	
	LEF-pyrogallol	C	0.04463	-10.93	-11.27	

Lenalidomide (LEN)	LEN-hemihydrate	P/H	0.65	-11.89	-10.85	[25]
	LEN-acesulfame	S	1.35	-18.62	-17.39	
Riluzole (RZ)	RZ	P	0.35	-13.39	-12.86	[26]
	RZ-glutaric acid	C	0.62	-18.87	-17.38	
	RZ-sorbic acid	C	1.98	-10.64	-10.82	
	RZ-malonic acid	S	3.21	-10.39	-10.83	
Sulfametoxazole (SMZ)	SMZ-form I	P	0.705	-27.84	-23.42	[27]
	SMZ-form II	P	1.447	-23.91	-20.74	
	SMZ-benzamidine	S	3.289	-6.56	-7.11	
	SMZ-1,2-di(4-pyridyl)ethylene	C	0.334	-12.43	-10.50	
Teriflunomide (TFM)	TFM	P	0.637	-9.93	-8.66	[28]
	TFM-diethanolamine	S	1.785	-7.16	-7.62	
	TFM-monoethanolamine	S	4.202	-11.68	-9.97	
Telmisartan (TEL)	TEL	P	0.07	-39.72	-40.75	[29]
	TEL-gentisic acid	C	0.26	-21.62	-23.71	
Tinidazole (TNZ)	TMZ-salicylic acid	C	3.807	-20.11	-17.16	[30]
Zonisamide (ZNS)	ZNS	P	0.8466	-24.42	-20.12	[31]
	ZNS-caffeine	C	0.7418	-7.00	-9.4	

For better visualization, the data were grouped by drug and in alphabetical order.
P=pure; C=cocrystal; S=salt and H=hydrate
** Solubility data were standardized in mg mL^{-1}.*

Calculation: $$\bar{E}_{framework} = \frac{\sum(E_{total}\, x\, n°_{interactions'\ type})}{N°_{Total\ interactions}}$$

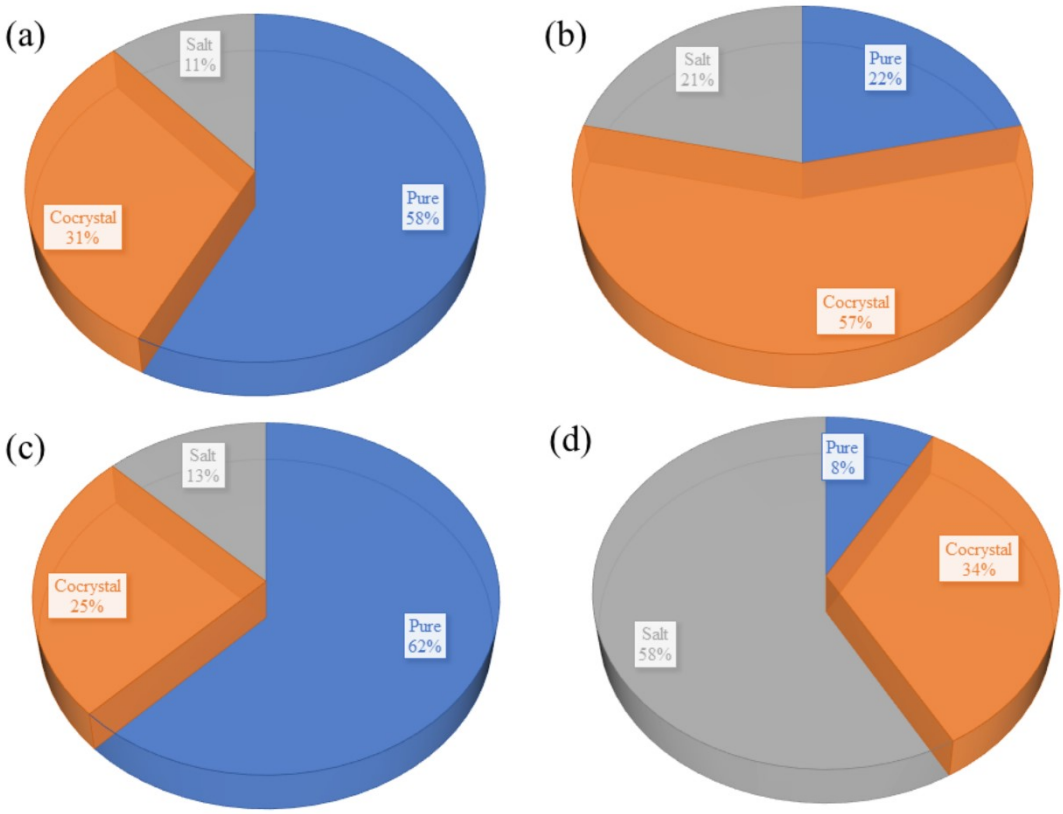

Figure S2. Distribution of the 60 solid forms selected in the four solubility ranges: (a) less than 0.10 mg mL^{-1}; (b) from 0.10 to 0.50 mg mL^{-1}; (c) from 0.50 to 1.00 mg mL^{-1} and (d) from 1.00 to 5.00 mg mL^{-1}.

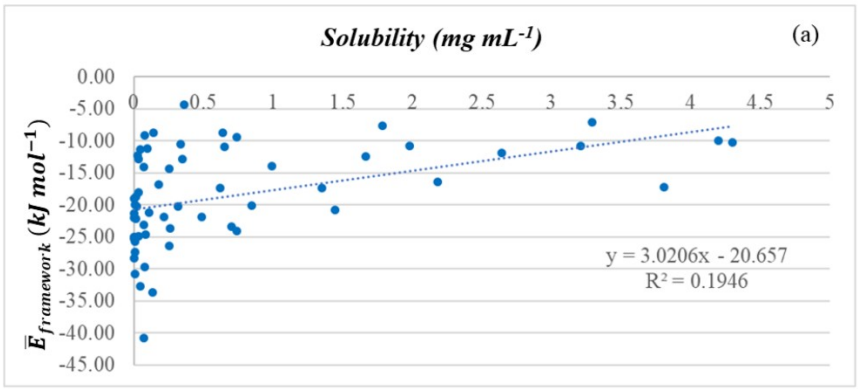

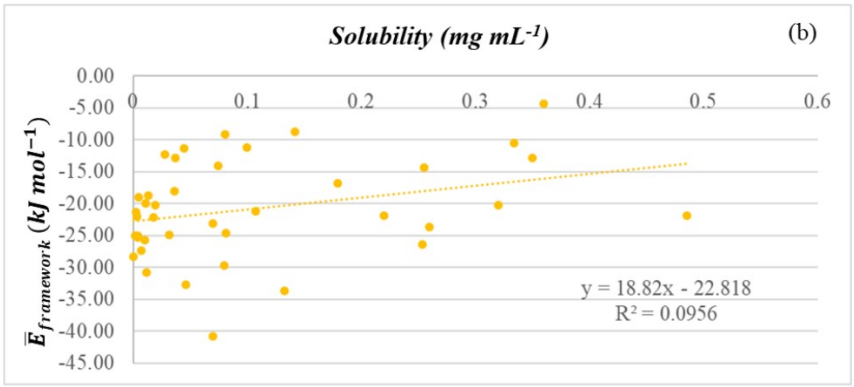

Figure S3. Linear representation of solubility and average of energy framework ($\bar{E}_{framework}$) for 60 solid forms investigated a) showing the dispersion of points a) within the entire range of solubility studied (0.00006 - 4.3 mg mL^{-1}) and b) only in the range of greatest variability between the points (≤ 0.5 mg mL^{-1}). The energy values were obtained at the B3LYP/6-31G(d,p) level.

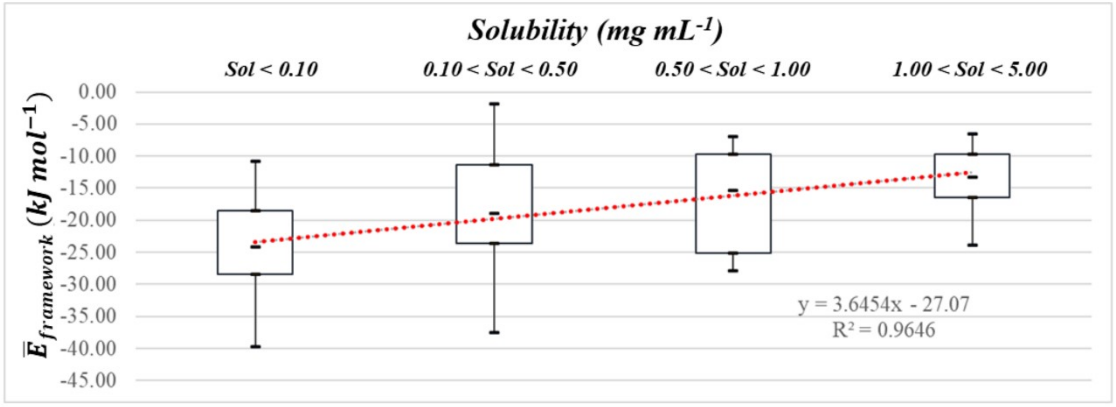

Figure S4. Box plot representation of solubility and average of energy framework ($\bar{E}_{framework}$) for 60 solid forms investigated. The energy values were obtained at the HF/3-21G level.

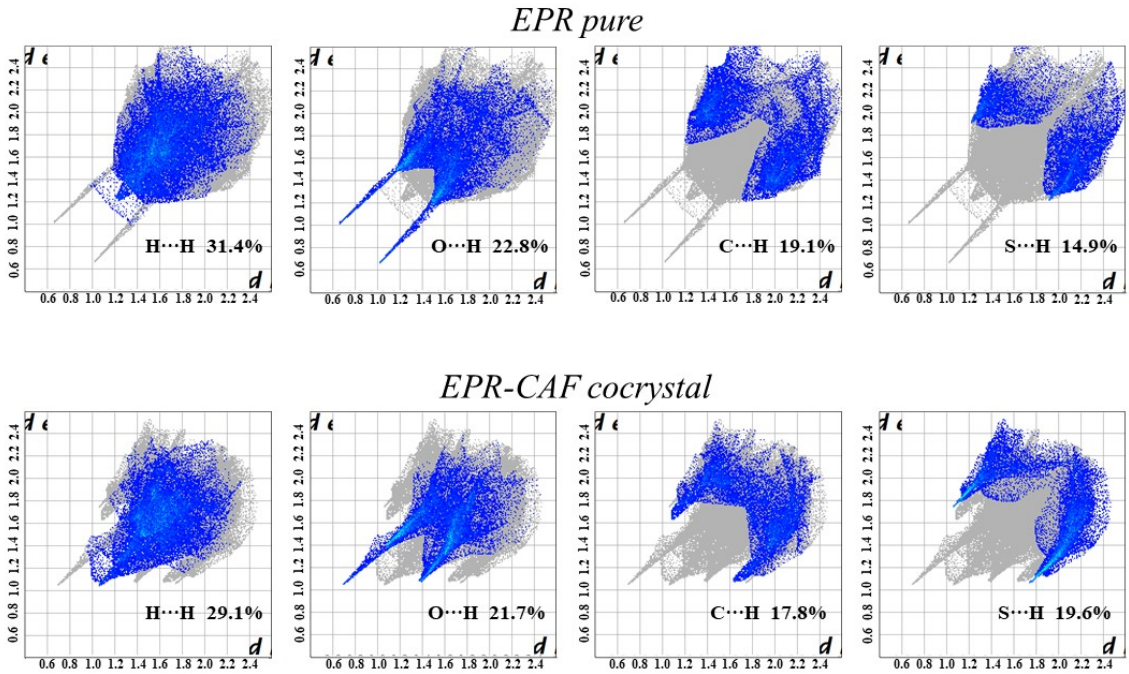

Figure S5. Partial fingerprint plots showing the percentual contributions of the main intermolecular contacts to the Hirshfeld surface area of the forms EPR (pure) and EPR-CAF cocrystal.

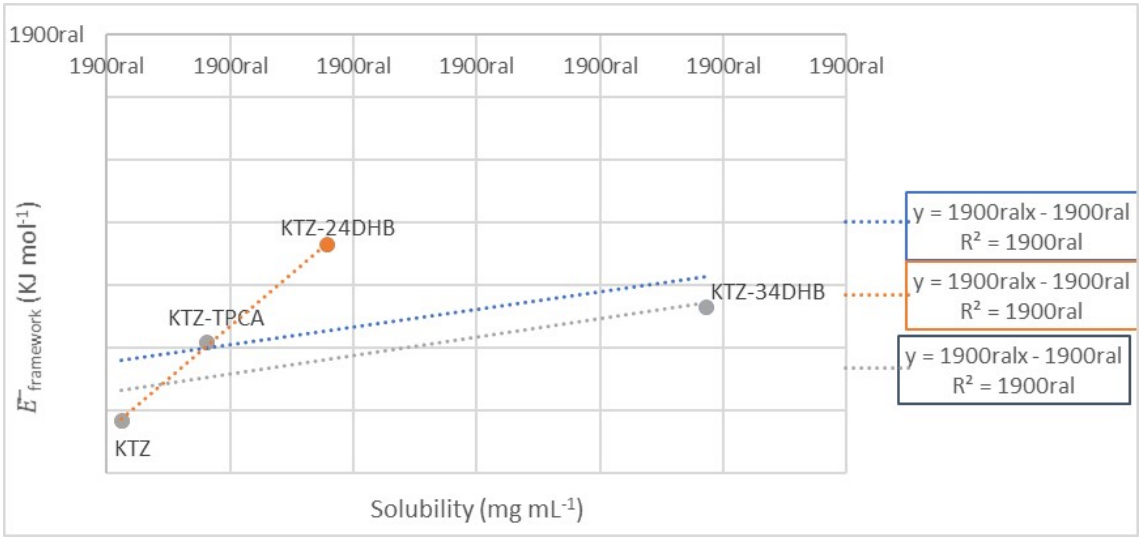

Figure S6. Correlation between the $E_{framework}$ and aqueous solubility for the four solid forms of ketoconazole studied. *The blue dotted line corresponds to the linear trend between the 4 points; the orange dotted line represents the linear trend for the first three points (KTZ; KTZ-TPCA and KTZ-24DHB) and the gray dotted line corresponds to the linear trend between KTZ; KTZ-TPCA and KTZ-34DHB).*

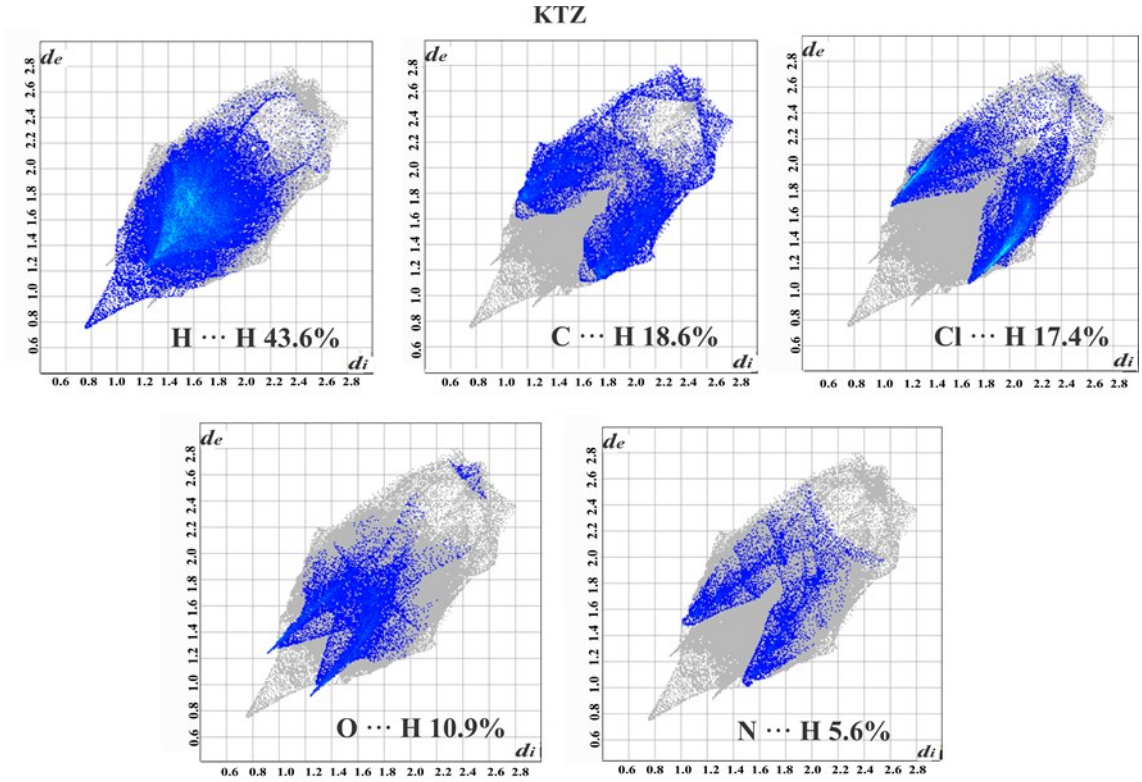

Figure S7. 2-D fingerprint plots of the KTZ structure showing the main contributions from specific pairs of atom-types.

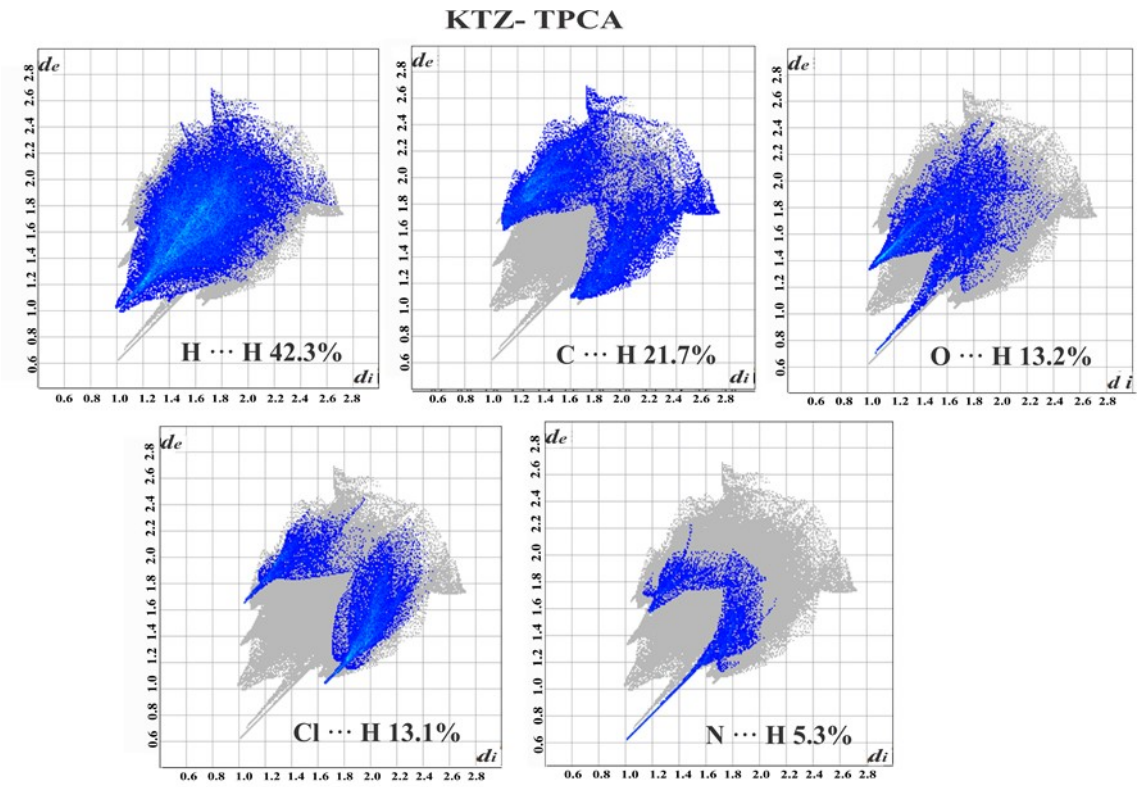

Figure S8. 2-D fingerprint plots of the KTZ-TPCA structure showing the main contributions from specific pairs of atom-types.

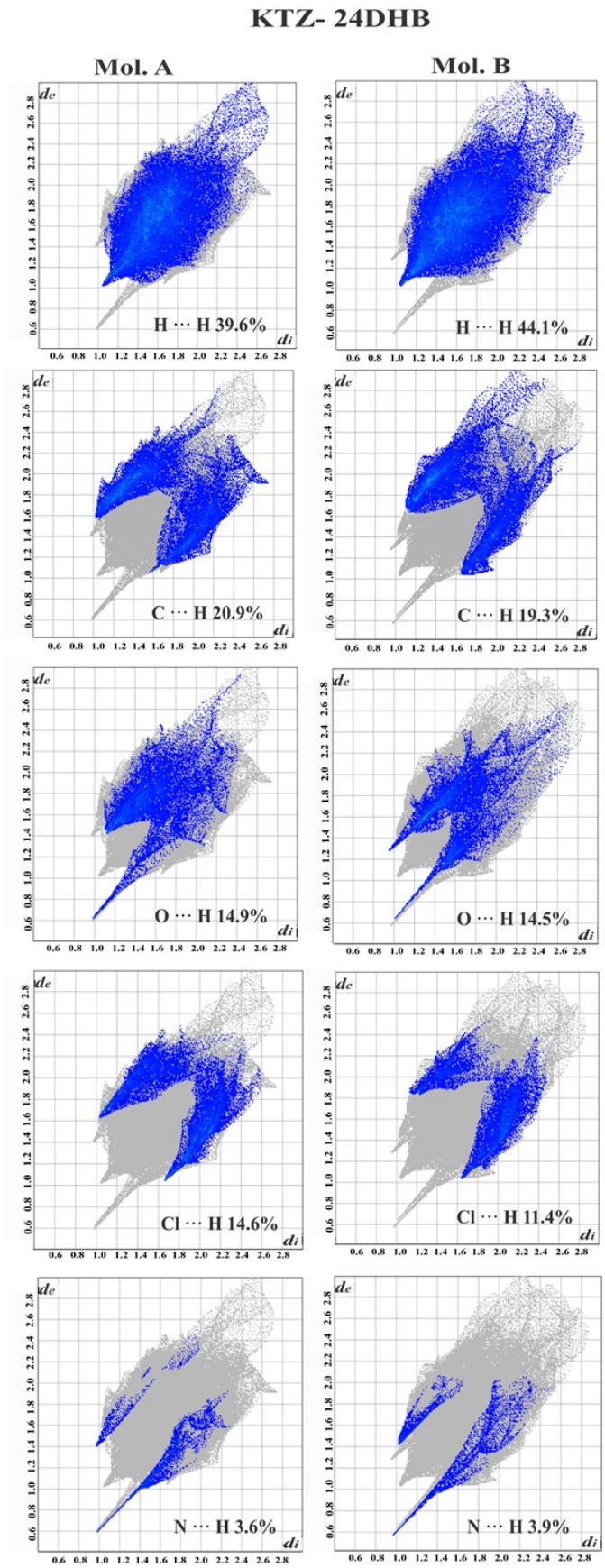

Figure S9. 2-D fingerprint plots for a) molecule A and b) molecule B of the KTZ-24DHB structure showing the main contributions from specific pairs of atom-types.

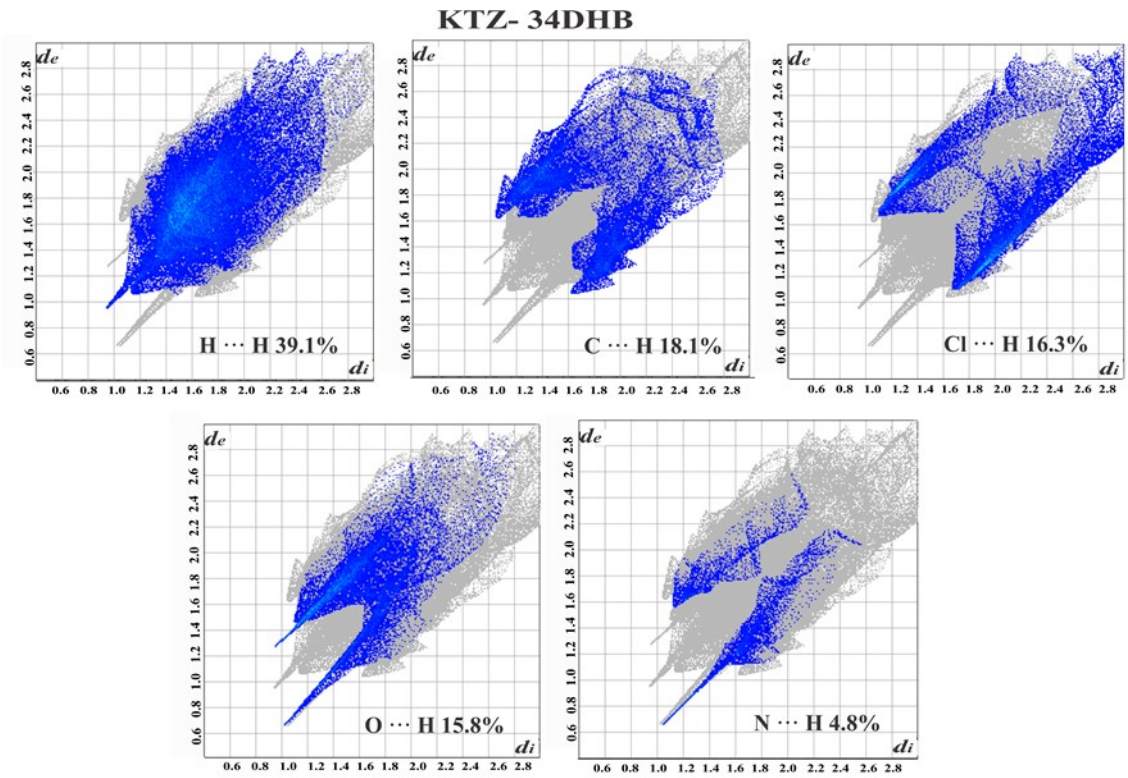

Figure S10. 2-D fingerprint plots of the KTZ-34DHB structure showing the main contributions from specific pairs of atom-types.

References

1 Y. X. Zhang, L. Y. Wang, J. K. Dai, F. Liu, Y. T. Li, Z. Y. Wu and C. W. Yan, *J. Mol. Struct.,* 2019, **1184**, 225–232.

2 Y. Song, L. Y. Wang, F. Liu, Y. T. Li, Z. Y. Wu and C. W. Yan, *CrystEngComm*., 2019, **21**, 3064–3073.

3 A. Bongioanni, M. S. Bueno, J. Abraham-Miranda, A. K. Chattah, A. P. Ayala, M. R. Longhi and C. Garnero, *Cryst. Growth Des.,* 2019, **19**, 4538–4545.

4 B. Zhu, J. R. Wang, Q. Zhang, M. Li, C. Guo, G. Ren, and X. Mei, *Cryst. Growth Des.,* 2018, **18**, 4701–4714.

5 F. Y. Wang, Q. Zhang, Z. Zhang, X. Gong, J. R. Wang, X. Mei, *CrystEngComm.,* 2018, **20**, 5945–5948.

6 M. Yoshimura, M. Miyake, T. Kawato, M. Bando, M. Toda, Y. Kato, T. Fukami and T. Ozeki, *Cryst. Growth Des.,* 2017, **17**, 550–557.

7 M. Aljohani, A. R. Pallipurath, P. McArdle and A. Erxleben, *Cryst. Growth Des.,* 2017, **17**, 5223–5232.

8 E. V. Gonzaga, S. S. Vieira, J. L. J. Vilaca, M. Guerra, M. G. Evangelista, I. M. L. Rosa, M.M. Figueiredo, O. M. M. S. Viana and A. C. Doriguetto, *Cryst. Growth Des.*, 2019, **19**, 737–746.

9 A. Ainurofiq, R.Mauludin, D. Mudhakir, D. Umeda, S. N. Soewandhi, O. D. Putra and E. Yonemochi, *Eur. J. Pharm. Sci*. 2018, **111**, 65–72.

10 W. Guo, S. Du, Y. Lin, B. Lu, C. Yang, J. Wang and Y. Zeng, *New J. Chem.*, 2018, **42**, 15068–15078.

11 M. K. Bommaka, M. K. C. Mannava, K. Suresh, A. Gunnam and A. Nangia, *Cryst. Growth Des.,* 2018, **18**, 6061–6069.

12 O. D. Putra, D. Umeda, Y. P. Nugraha, T. Furuishi, H. Nagase, K. Fukuzawa, H. Uekusa and E. Yonemochi, *CrystEngComm*., 2017, **19**, 2614–2622.

13 O. D. Putra, D. Umeda, Y. P. Nugraha, K. Nango, E. Yonemochi and H. Uekusa, *Cryst. Growth Des.*, 2018, **18**, 373–379.

14 Y. Kang, J. Gu and X. Hu, *J. Mol. Struct.,* 2017, **1130**, 480–486.

15 X. R. Zhang and L. Zhang, *J. Mol. Struct.,* 2017, **1137**, 328–334.

16 L. Gao, X. R. Zhang, Y. F. Chen, Z. L. Liao, Y. Q. Wang and X. Y. Zou, *J. Mol. Struct.*, 2019, **1176**, 633–640.

17 L. F. Diniz, P. S. Carvalho, S. A. C. Pena, J. E. Gonçalves, M. A. C. Souza, J. D. de Souza Filho, L. F. O. Bomfim Filho, C. H. J. Franco, R. Diniz and C. Fernandes, *Int J Pharm,* 2020, **587**, 119694.

18 J. A. Miranda, C. Garnero, A. K. Chattah, Y. S. Oliveira, A. P. Ayala and M. R. Longhi, *Cryst. Growth Des.*, 2019, **19**, 2060–2068.

19 P. Goyal, D. Rani and R. Chadha, *Cryst. Growth Des.*, 2018, **18**, 105–118.

20 A. L. M. Viana, A. C. Doriguetto, O. M. M. S. Viana, A. L. M. Ruela, J. T. J. Freitas, B. E. M. Souto, M. B. Araújo and F. B. A. Paula, *Int. J. Pharm.*, 2018, **553**, 272–280.

21 L. Y. Wang, F. Z. Bu, Y. T. Li, Z. Y. Wu, C. W. Yan, *Cryst. Growth Des.*, 2020, **20**, 3236–3246.

22 Q. Fu, H. D. Lu, Y. F. Xie, J. Y. Liu, Y. Han, N, B. Gong and F. Guo, *J. Mol. Struct.,* 2019, **1185**, 281–289.

23 X. Chen, D. Li, Z. Deng and H. Zhang, *Cryst. Growth Des.,* 2020, **20**, 6973–6982.

24 J. Cadden, W. T. Klooster, S. J. Coles and S. Aitipamula, *Cryst. Growth Des.*, 2019, **19**, 3923–3933.

25 X. Chen, D. Li, J. Wang, Z. Deng and H. Zhang, *J. Mol. Struct.*, 2019, **1175**, 852–857.

26 P. K. Mondal, V. Rao, S. Mittapalli and D. Chopra, *Cryst. Growth Des.*, 2017, **17**, 1938–1946.

27 M. Alsubaie, M. Aljohani, A. Erxleben and P. McArdle, *Cryst. Growth Des.*, 2018, **18**, 3902–3912.

28 A. Gunnam and A. K, Nangia, *Cryst. Growth Des.,* 2019, **19**, 5407–5417.

29 J. Haneef, P. Arora and R. Chadha, *AAPS PharmSciTech*., 2020, **21**. DOI: 10.1208/s12249-019-1559-9.

30 O. E. Fandiño, L. Reviglio, Y. G. Linck, G. A. Monti, M. M. Marcos Valdez, S.N. Faudone, M.R. Caira and N. R. Sperandeo, *Cryst. Growth Des.*, 2020, **20**, 2930–2942.

31 S. Aitipamula, J. Cadden and P. S. Chow, *CrystEngComm.*, 2018; **20**, 2923–2931.